ARTÍCULO ORIGINAL

Gac Méd Caracas 2022;130(2):323-338
DOI: 10.47307/GMC.2022.130.2.11

Rue and clove microspheres: antiamebic activity, hemocompatibility, and release kinetics

Microesferas de ruda y clavo: actividad antiamébica, hemocompatibilidad y cinética de liberación

Euridice Ladisu Mejía-Argueta[1], Jonnathan Guadalupe Santillán-Benítez[2*], Miriam Flores-Merino[3], Claudia Cervantes-Rebolledo[4], Mario Nequiz-Avendaño[5]

SUMMARY

Objectives: *The alginate microspheres were prepared with methanol extract of rue and essential oil of clove with metronidazole evaluating their biological and physicochemical activities.* **Materials and methods:** *Microspheres were evaluated with their sphericity, encapsulation efficiency, degradation, and release kinetics with mathematical models. Also, their hemocompatibility and antiamebic activity were studied on hemolytic, proteolytic, and erythrophagocytic activities of Entamoeba histolytica.* **Results:** *Microspheres were obtained with sphericity equal to one, with encapsulation efficiency greater than 50 % (except CEO in 220 nm). Their degradation was recorded between 8 %-12 % in acidic and basic pH. In addition, its release kinetics had a burst constant in almost all the treatments, with the behavior of Korsmeyer-Peppas and Peppas-Sahlin being of pseudofickian behavior. The microspheres were hemocompatible according to the regulations (<10 %) and additionally decreased virulence factors of the amoeba such as hemolytic, proteolytic, erythrophagocytic activities.* **Conclusions:** *The microspheres obtained could be a possible treatment against E. histolytica. Still, other toxicity parameters have to be determined (i.e., cytotoxicity, cytocompatibility, biosafety, body weight, survival rate, weight index of main organs, histopathology of main organs, serum biochemical, etc.), as well as physicochemical parameters such as differential scanning calorimetry, Fourier-transform infrared spectroscopy and viscosity.*

Keywords: *Alginate, drug release, herbal compounds, microspheres, parasitic activities.*

RESUMEN

Objetivos: *Se prepararon microesferas de alginato con extracto de metanol de ruda y aceite esencial de clavo con metronidazol evaluando sus actividades biológicas*

DOI: https://doi.org/10.47307/GMC.2022.130.2.11

ORCID: 0000-0003-0137-498X[1]
ORCID: 0000-0003-3574-1231[2]
ORCID: 0000-0003-0793-0940[3]
ORCID: 0000-0001-5914-3047[4]
ORCID: 0000-0003-2818-2267[5]

[1,2*]Autonomous University of the State of Mexico (UAEMex). Toluca, Mexico. Toxicology Laboratory, Pharmacy Department, Faculty of Chemistry, UAEMex. Zipcode: 50120. E-mail: qfb.elma@hotmail.com

[3]Autonomous University of the State of Mexico (UAEMex). Experimental Chemistry Laboratory, Faculty of Chemistry. UAEMex. Toluca, Mexico Zipcode: 50120. E-mail: mvfloresm@uaemex.mx

[4] UICUI. Ixtlahuaca, State of Mexico. Zipcode: 50740. E-mail: claudiacervantes@uicui.edu.mx

[5] National Autonomous University of Mexico (UNAM). Experimental Medicine Research Unit, Faculty of Medicine and General Hospital "Dr. Eduardo Liceaga". Zipcode: 067720. E-mail: manequiz@yahoo.com.mx

*Corresponding author: Jonnathan Santillán-Benítez. E-mail: jonnathangsb@yahoo.com.mx

Recibido: 27 de marzo 2022
Aceptado: 12 de abril 2022

y fisicoquímicas. **Materiales y métodos:** *Se evaluó su esfericidad, eficiencia de encapsulación, degradación y cinética de liberación con modelos matemáticos. También se estudió su hemocompatibilidad y actividad antiamébica sobre las actividades hemolítica, proteolítica y eritrofagocítica de Entamoeba histolytica.*
Resultados: *Se obtuvieron microesferas con esfericidad igual a uno, con una eficacia de encapsulación superior al 50 % (excepto el CEO en 220 nm). Su degradación se registró entre el 8 %-12 % en pH ácido y básico. Además, su cinética de liberación tuvo una constante de estallido en casi todos los tratamientos, siendo el comportamiento de Korsmeyer-Peppas y Peppas-Sahlin de comportamiento pseudofictico. Las microesferas fueron hemocompatibles según la normativa (<10 %) y además disminuyeron los factores de virulencia de la ameba como las actividades hemolíticas, proteolítica y eritrofagocítica.* **Conclusiones:** *Las microesferas obtenidas podrían ser posiblemente empleadas en el tratamiento contra E. histolytica. Queda aún por determinar otros parámetros de toxicidad (es decir, citotoxicidad, citocompatibilidad, bioseguridad, peso corporal, tasa de supervivencia, índice de peso de los órganos principales, histopatología de los órganos principales, bioquímica sérica, etc.), así como parámetros fisicoquímicos tales como la calorimetría diferencial de barrido, espectroscopia infrarroja con transformación de Fourier y la viscosidad.*

Palabras clave: *Alginato, liberación de fármacos, compuestos herbales, microesferas, actividades parasitarias.*

RESUMO

La corrección para esta parte sería por favor para evitar la duplicidad del resumen en español:
Objetivos: *As microesferas de alginato foram preparadas com extracto de metanol de arruda e óleo essencial de cravo com metronidazol avaliando as suas actividades biológicas e físico-químicas. Materiais e métodos: Foram avaliados com a sua esfericidade, eficiência de encapsulamento, degradação, e cinética de liberação com modelos matemáticos. Além disso, sua hemocompatibilidade e atividade antiamebiana foram estudadas nas atividades hemolítica, proteolítica e eritrofagocitária da Entamoeba histolytica.*
Resultados: *Foram obtidas microesferas com esfericidade igual a um, com eficiência de encapsulamento superior a 50 % (exceto CEO em 220 nm). Sua degradação foi registrada entre 8-12% em pH ácido e básico. Além disso, sua cinética de liberação teve uma rotura constante em quase todos os tratamentos, sendo o comportamento de Korsmeyer-Peppas e Peppas-Sahlin de comportamento pseudofickiano. As microesferas foram hemocompatíveis de acordo com os regulamentos (<10%) e, adicionalmente, diminuindo os fatores de virulência da ameba, como atividades hemolíticas, proteolíticas e eritrofagocitárias.* **Conclusões:** *Portanto, as microesferas obtidas podem ser um possível tratamento contra E. histolytica. Ainda assim, devem ser determinados outros parâmetros de toxicidade (ou seja, citotoxicidade, citocompatibilidade, biossegurança, peso corporal, risco de mortalidade, índice de peso multiorgânico, histopatologia dos danos dos órgãos, bioquímica do soro, etc.). E parâmetros físico-químicos (ou seja, calorimetria exploratória diferencial, espectroscopia infravermelha com transformada de Fourier, viscosidade).*

Palavras-chave: *alginato, liberação de drogas, compostos de ervas, microesferas, atividades parasitárias.*

INTRODUCTION

Microencapsulation is a technique that favors the protection and retention of liquid, solid and gaseous substances employing a polymer such as sodium alginate, which forms a wall that prevents the active ingredient from volatilizing, degrading, or reacting with other substances (1). This is a process where small particles or droplets are surrounded by a homogeneous or heterogeneous coating integrated into capsules with various applications. It is the technique of obtaining a barrier that delays chemical reactions with the surrounding medium, increasing the product's shelf life. The gradual release of the encapsulated compound, and even facilitating its handling by converting a liquid or gaseous material into a solid form called a microcapsule, which consists of a spherical, semi-permeable, thin, and robust membrane surrounding a solid or liquid core, with a diameter varying from a few microns to 1 000 μm. Microspheres are multiparticulate drug delivery systems which are prepared to obtain prolonged or controlled drug delivery to improve bioavailability, stability and target the drug to a specific site at a predetermined rate. The core that makes up the microcapsule is also called the inner phase or active ingredient, just as the membrane can be referred to as the outer layer or matrix (2).

Hydrocolloids have been used as a matrix due to their ability to absorb water, ease of handling, and safety. Alginate is a hydrocolloid that possesses these characteristics and gelling, stabilizing, and thickening properties. It is also described as a hydrophilic linear polyionic polysaccharide from marine algae with two monomers in its structure, α-L-guluronic acid (G) and β-D-mannuronic acid (M), which are distributed in sections constituting homopolymers type G-blocks (-GGG-), M-blocks (-MMM-) or heteropolymers where the M and G block alternate (-MGMG-). Both the distribution of its monomers in the polymer chain and the charge and volume of the carboxylic groups give the gel-formed characteristics of flexibility or rigidity depending on the G content (3).

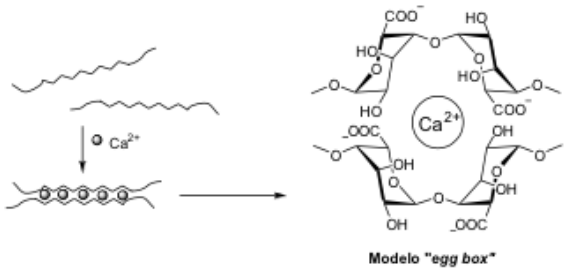

Figure 1. Mechanism of sodium alginate with $CaCl_2$ forming the egg case.

The gelation process occurs in multivalent cations (except magnesium), where the food industry uses the calcium ion most. Gelation occurs when a binding zone between a G-block of an alginate molecule physically binds to another G-block contained in another alginate molecule via the calcium ion (Figure 1) (3). Sodium alginate is a biodegradable and biocompatible polymer composed of brown algae that act as a stabilizer, binder, and thickener. It can provide a controlled or immediate release of the encapsulated active ingredient in gel form (4).

It also avoids the oxidation/degradation phenomena of natural products, improves their shelf life, prolongs their antioxidant efficacy phenolic compounds, adds nutritional value and biological properties, and is used in different techniques for obtaining microspheres of microencapsulated products in the cosmetic, food, and pharmaceutical industries. This kind of research opens the door to a line of research already studied before based on pharmacognosy and phytochemistry to extract secondary metabolites from plants for uses such as adjuvants and preservatives, among others (5-7).

Biocompatibility testing is a strategy to evaluate materials to regenerate functional tissues. In this strategy, pathophysiological processes are studied *in vivo* and *in vitro* by selecting cells and materials according to the metabolic and mechanical conditions of the area to be repaired. Therefore, biomaterials must have specific properties and characteristics to repair the surface. The biocompatibility process is so necessary that studies in this field must be carried out following the International Organisation for Standardisation (ISO), following the international guide ISO-10993 (biocompatibility studies) (8).

Some studies have been conducted on secondary metabolites of medicinal plants in microspheres such as rutin, camptothecin, silymarin, turmeric oil, gallic acid, and astaxanthin (9-11). These studies helped to consider the encapsulation efficiency, the particle size, and the mathematical models that demonstrated the behavior in the release kinetics. Likewise, other studies mentioned the potential antiamoebic activity of plants. In this sense, it was shown high antiprotozoal activity on *Entamoeba histolytica* trophozoites employing *in vitro* tests with rue methanolic extract and its fractions as n-hexane, EtOAc, $CHCl_3$-EtOAc, and with pancreas extract or *Larrea tridentate* (ethanolic extract; lignan; IC_{50}=186.2 μg/mL), *Persea americana* (ethanolic extract; glycosides and lignan; IC_{50}=296.94 μg/mL), *Piper longum* (butanol and chloroform extract; coumaparine; IC_{50}=186.2 μg/mL), among other studies performed with the crude extracts or secondary metabolites isolated without encapsulation and other parasitic activities such as proteolytic, hemolytic, erythrophagocytosis (12-14).

The above-mentioned herbal metabolites are essential for some microbial as *E. histolytica* which produces human amoebiasis (amebomas, chronic colitis, hepatic abscess), a disease-causing

significant morbidity and mortality worldwide, being the second leading cause of death caused by protozoan parasites (15). Moreover, its treatment with metronidazole (MZL), is not effective against luminal trophozoites producing a slow response and treatment failures, and has been reported and has secondary effects (i.e., metallic taste, headache, teratogenicity, etc.) (16). The aim of the present study is to obtain and evaluate rue and clove microspheres alone and combined with metronidazole. Their hemolytic, proteolytic, and erythrophagocytic activities on *Entamoeba histolytica* were assessed, and their hemocompatibility, release kinetics, and other parameters were studied to be used adjuvants with metronidazole and to reduce their adverse effects in prolonged treatments.

It has been established that in order to approve as a drug for human use and determine its shelf life, and stability, it is necessary to elucidate the possible mechanism of kinetic release of the herbal metabolites in accordance to Guidance for Industry Q1A(R2) Stability Testing of New Drug Substances and Products from the USFDA in 2003 (17,18).

MATERIALS AND METHODS

Microencapsulation

Ruta chalepensis was macerated in methanol and reduced using a rotary evaporator, and *Syzygium aromaticum* was macerated in distilled water overnight and hydrodistilled, both collected in El Oro, State of Mexico (Mexico). For alginate emulsions with the selected extract and essential oil were prepared with a solution of sodium alginate (DAHIPRO, 1.5 % w/v) and $CaCl_2$ (DAHIPRO, 1.3 % w/v) by dilution in distilled water at 35°C. Each dilution was left to stir at 200 rpm on a magnetic stirrer for 2 hours (19,20). Different emulsions were prepared by mixing clove essential oil or extract with metronidazole and alginate. The formulations and final concentrations were a) 240 mg/mL of essential oil (CEO), b) 240 mg/mL essential oil with 0.05 mg/mL metronidazole (CEO+MZL), c) 100 mg/mL of extract (RE) and d) 100 mg/mL of extract with 0.05 mg/mL metronidazole (RE+MZL) (the concentration of essential oil or extract was determined in a growth inhibition kinetics in a previous test (no data showed).

After the solutions were obtained, they were extruded with a syringe through a 10 mL pipette and dripped into a $CaCl_2$ solution. The tip of the needle was set 10 cm above the surface of the gelling bath. The drop rate was set at 30 drops per minute. $CaCl_2$ gelling solution (1.3 % w/v) formed microspheres loaded with the extract and essential oil with and without metronidazole. Subsequently, microspheres were filtered using a Kitasato flask, a Büchner funnel, and a vacuum pump (VDE 0530, KNF Neuberger GmbH, Germany), sieved, and dried in an oven at 40°C for 12 h and observed under a phase-contrast microscope.

Phase-contrast imaging

Samples were analyzed in an inverted-phase contrast microscope TCM 400 (LABOMED, China). For this purpose, samples were placed on glass slides and visualized at magnifications of 4, 20, and 40x (21,22).

Encapsulation efficiency

To determine the EE %, accurately weighed amounts (200 mg) of microcapsules were suspended in 30 mL phosphate buffer (pH=7.4) and stirred at 150 rpm at room temperature until the complete dissolution of microcapsules. Then, the solution was centrifuged at 9000 rpm for 5 min, and the total content was determined in the supernatant using a UV-VIS spectrometer. EE% was calculated using the following equation 1 (23):

$$EE\ (\%) = \frac{(Total\ amount\ of\ loaded\ active\ principle)}{(Initial\ amount\ of\ active\ principle)} \times 100$$

(Eq. 1)

Degradation of the beads

The degradation of these materials was analyzed after they reached their maximum weight loss in PBS solution (pH=7.4) and diluted HCl (pH=1.2) for 14 d. Finally, the degradation rate of all materials was measured as the degradation ratio (DR) until the total weight of the sample became stable. Three replicate experiments were performed, and the maximum weight loss was set as 100 %. The DR was calculated according to the following equation (24):

$$DR = \frac{(W\_s)-W)}{(W\_ms-W)} \times 100\ \% \quad W\_ms = \text{weight of tubes in maximal loss after removing the supernatant}$$

(Eq. 2)

Release kinetics

The released extract or essential oil alone and combined were quantified spectrophotometrically at 220, 300, and 320 nm for the oil and the extract at 210, 300, and 320 nm; these wavelengths were determined for the maximum peaks for the herbal products using IMPLEN NanoPhotometer (no data showed). The release was tested using a dissolver (PT-DDS4 - Pharma Test). Briefly, five microspheres were tested per treatment at a pH=1.2 (2 g NaCl in 7 mL HCl concentrated) and pH=7.4 (Na_2HPO_4 and NaH_2PO_4), making aliquots at 5, 10, 20, 30, 30, 40, 60, 90, and 120 min using the paddle method (method II) in a previously calibrated dissolver. The stirring speed of the paddles was 75 rpm at a temperature of 37 ± 0.5 °C in a 900 mL beaker, taking aliquots of 3 mL at each time without recovering the buffer (25-27).

In addition, mathematical modeling of the release kinetics occupied for our study was Zero order, first order, Korsmeyer-Peppas, Peppas-Sahlin, Weibull, and was carried out as follows.

Order 0: This is a widely used model for dosage systems that do not disaggregate, making the drug release very slow. This model assumes that the tablet area does not change considerably and that no material equilibrium conditions are formed. Expressed from the following equation:

$$Q\_t = Q\_0 + (k\_0)t \quad \text{(Eq. 3)}$$

Q_t is the amount of drug dissolved at time t, Q_0 is the initial amount of drug in solution (most of the time $Q_0 = 0$), and k_0 corresponds to the zero-order release constant (28).

Order 1: This model describes the absorption and release of some drugs from porous matrices. The following equation can express the release of drugs following this kinetics:

$$LogC_t = LogC_0 - \frac{k_1}{2.303}t \quad \text{(Eq. 4)}$$

C_t is the amount of drug remaining at time t, C_0 is the initial drug in solution, and k_1 is the first-order release constant. As the amount of drug in the solid-state decreases, the concentration of the dissolution medium is enriched with the solute, so the release process is conditioned by the saturation point of the solute (28).

Korsmeyer-Peppas's model explains drug release mechanisms where erosion and dissolution of the matrix occur, a generalized model of the Higuchi equation. It has been widely used to describe drug release from polymeric systems. The equation is as follows:

$$\frac{M_t}{M_\infty} = K_r t^n \quad \text{(Eq. 5)}$$

Where M_t/M_∞ corresponds to the fraction of drug released at time t; K_r is the release counter characteristic for polymer-drug interactions, while n is equal to the diffusion exponent characteristic of the release mechanism. A value of n equal to 0.5 indicates that the drug release mechanism is Fickian; values between 0.5 and 1 indicate a non-Fickian release mechanism, while n equal to 1 suggests that the mechanism is like zero-order release kinetics. For values greater than 1, drug release depends on the relaxation of

the polymer chains in the matrix from a glassy to a rubbery state with higher kinetic motion. The determination of the exponent n should be performed with 60 % of the drug dissolved (29).

Peppas-Sahlin: In the thin-film system (planar geometry), the release mechanism can be classified as Fickian diffusion ($n \leq 0.5$), non-Fickian (anomalous) diffusion ($0.5 < n < 1$), and Case II diffusion ($n = 1$), depending on the n values. The following equation describes this model:

$$\frac{M_t}{M_\infty} = K_d t^m + K_r t^{am} \text{ (Eq. 6)}$$

M_t/M_∞ is the fraction of drug released at time t, K_d is the Fickian kinetic constant, K_r is the erosion rate constant, and m is the Fickian diffusion exponent. The release mechanism can be classified as diffusion ($|K_d / K_r| > 1$), erosion (or relaxation) ($|K_d / K_r| < 1$), and coexistence of diffusion and erosion ($|K_d / K_r| = 1$), according to the relation ($|K_d / K_r|$) (30,31).

Weibull: It has been applied to many mechanisms to study the kinetics of heterogeneous processes and to fit drug release by nanosystems which follows the following equation:

$$Q_t = (100 - Q_0)\left|1 - e^{\left(\frac{t}{T_d}\right)^\beta}\right| \text{ (Eq. 7)}$$

Q_0 is release time; Q_t is % drug released at time t; T_d, time after the release of 63.2 % of the drug from the formulation; β , shape parameter in the Weibull model; *a*, *b*, slope and intersection of the graph representing the release process (32,33).

Sterility test

The microspheres were placed in sterile vials and the laminar flow hood for 10 min in UV light. Sterility of the microspheres was confirmed by incubating a portion of the sterile batch at an incubation T of 37 °C in nutrient broth for 5 d, where the sterility was approved when there was no turbidity or color change in a nutrient medium (27,34).

Haemocompatibility *in vitro*

Before testing, bead samples were sterilized with UV light in a laminar flow hood. Hemolysis and platelet activation tests were performed, and leukocyte degranulation and viability tests were (35).

Blood samples were collected from healthy volunteers in Vacutainer tubes containing heparin. Direct contact methods determine the hemolytic assay according to ISO 10 993-4 (1992) with general requirements for evaluating interactions of medical devices with blood based on the hemolytic activity of alginate beads.

Hemolysis test: Blood samples were centrifuged at 3 000 rpm for one minute, removed with a Pasteur pipette and washed with saline, centrifuged three times, and the total erythrocyte suspension was obtained. This suspension was incubated for one hour with one microsphere per treatment and control (H_2O distilled). This technique was obtained by measuring the absorbance at 415 nm and its spectrum in the range (200-600 nm) of the samples with their respective scans, using a spectrophotometer GENESYS 10S UV-Vis v4.002 2L5P026002, calculating the percentages of hemolysis, using the absorbance of the sample and the data of the controls.

Platelet activation test: Blood samples are centrifuged at 1200 rpm for 10 min to obtain platelet-rich plasma (PRP). The separation of blood elements was performed based on density. One microsphere was incubated per treatment with PRP for one h at 37°C under static conditions, then smeared and Wright stained. The percentage of platelet activation is based on the number of platelet aggregates observed under the microscope.

Leukocyte degranulation and viability test on mononuclear cells. Leucocytes were obtained by identifying the Buffy Coat (BC), which refers to the leukocyte-platelet layer immediately above the red layer, and was obtained by centrifuging

samples at 1 200 rpm for 10 min. This layer contained less than 1 % of the total volume of the blood sample and must therefore be handled carefully. The microspheres were incubated with the BC for one h at 37 °C under static conditions to contact the tested material. Wright staining of the smear was used to assess activity.

Erythrophagocytosis

Briefly, $100x10^6$ *E. histolytica* trophozoites were incubated with $500x10^6$ human erythrocytes (control) and the treatments (three microspheres per treatment) in 1 mL PBS for 15 min at 37 °C and then centrifuged at 500 ×g for 3 min. Non-phagocytosed erythrocytes were lysed by osmotic shock (0.4 mL of water) followed by 1 mL of PBS. The samples were then centrifuged at 14 000 ×g for 1 min. The pellet was clarified by adding 0,5 mL of formic acid followed by 0,5 mL PBS. The absorbance was determined at 397 nm in Lambda Bio+Spectrophotometer (PerkinElmer) (36).

Hemolytic activity

A total of $100x10^6$ *E. histolytica* trophozoites were incubated with 500×10^6 human erythrocytes (control), and the treatments (three microspheres per treatment) were incubated for one h at 37 °C in 1 mL PBS. After this time, the samples were centrifuged at 560 ×g for 3 min, and the absorbance of hemoglobin was determined. The absorbance of the hemoglobin in the supernatant was determined at 570 nm in Lambda Bio+Spectrophotometer (PerkinElmer) (36).

Proteolytic activity

Briefly, $100x10^6$ *E. histolytica* trophozoites were lysed by freezing in 0.2 mL PBS and 0.4 mL azocasein (2,5 mg/mL). The mixture was incubated for three h at 37 °C, and the reaction was stopped with 0,6 mL of trichloroacetic acid cold for 5 minutes at 4 500 g, and the absorbance was determined in the supernatant at 366 nm in Lambda Bio+Spectrophotometer (PerkinElmer) (37).

Statistical analysis

The data obtained represent the average of at least three different experiments ± standard deviation. ANOVA test with blocking and post hoc Tukey test was used for the degradation study. For release kinetics, was used three-way ANOVA. For hemocompatibility, ANOVA and post hoc Tukey tests were used, and hemolytic, proteolytic, erythrophagocytic activities were used Student t-test with paired samples. A $p<0.05$ was considered statistically significant, determining the normality using test Shapiro-Wilks, using InfoStat 2020. Data were presented as the mean ± SD of triplicate determinations and percent in graphs using Origin Pro 2019.

RESULTS

Microencapsulation and phase-contrast imaging

The mean diameter for the swollen microspheres was RE ($\overline{x}$ =3.9 mm ± 0.01), RE+MZL ($\overline{x}$ =2.4 mm ± 0.01), CEO ($\overline{x}$ =2.4 mm ± 0.05), and CEO+MZL ($\overline{x}$ =2.5 mm ± 0.04) using Image J 1.53k software, and a sphericity factor of 1 that were considered spherical (Figure 2).

Encapsulation efficiency and percent yield

The yield of the microspheres was determined by comparing the total weight of the microspheres obtained with the sum of the weight of the essential oil/methanolic extract and the polymers. In addition, UV-VIS spectra were determined to obtain the maximum peaks; RE (210, 300, and 320 nm) and CEO (220, 300, and 320 nm). The percentage yields of the optimized formulations ranged from 54 % to 81 %, with RE+MZL being the highest (Table 1). The method's loss of essential oil/methanolic extract may be due to the loss during the microspheres' hardening, washing, and filtering processes.

The encapsulation efficiency at the different wavelengths between 300 and 320 nm was found to be between 70 %-97 % and for the specific wavelengths for RE (71 %-94 %) and CEO (25 %-27 %), the latter being the lowest (Table 1). In

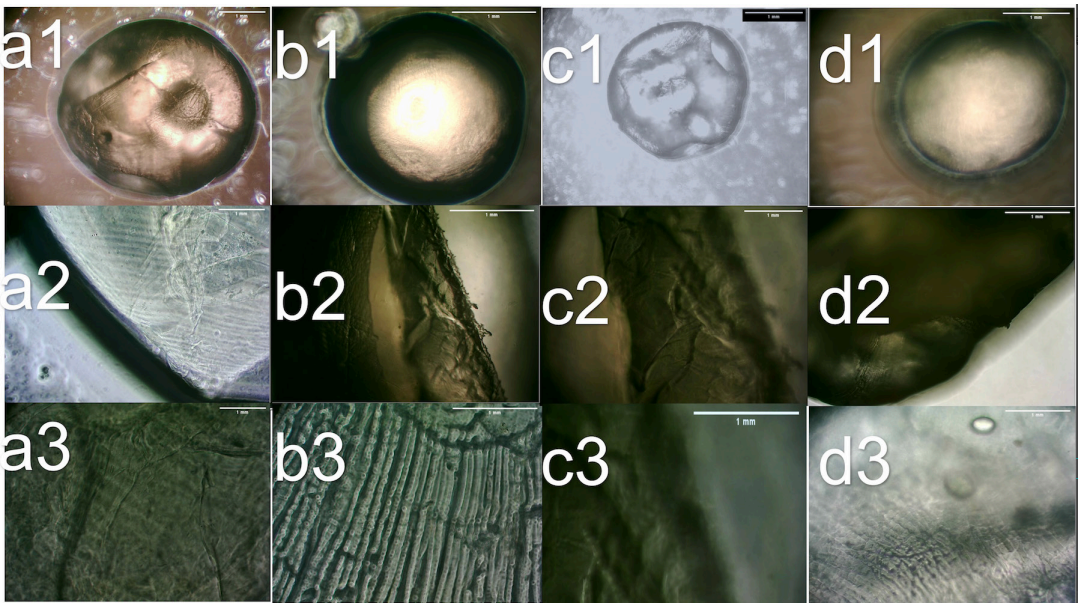

Figure 2. Optical micrographs. Where a is RE, b is RE+MZL, c is CEO and d is CEO+MZL. a1-d1 (surface of microsphere 4x); a2-d2 (surface of microsphere 20x); a3-d3 (surface of microsphere 40x).

this sense, the wavelength of 220 nm could be extended to other wavelengths, as in the study by da Silva (2021) (38). The maximum peak was found at 230 nm using UV-VIS, or several measurements could be made in different ranges with a bibliography where eugenol is presented at 280 nm or using standards of the secondary metabolites present in the essential oil. In turn, the CEO formulation would have to be supplemented with a surfactant or adding β-cyclodextrins (39) to re-evaluate this variable without significant differences and to complement the wavelengths obtained with abs-UV-Vis spectra as in the Radomski (2021) study (40,41). The above mentioned prove diverse factors and improve the formulation.

Table 1

Encapsulation efficiency percentage (EE %) and percent yield per treatment

Microspheres	% yield	% EE 210 nm	% EE 220 nm	% EE 300 nm	% EE 320 nm
RE+MZL	81.08	71.87±0.13	NA	72.21±0.00	52.94±0.00
RE	71.79	94.41±0.07	NA	97.84±0.00	74.62±0.00
CEO+MZL	54.60	NA	27.97±0.08	77.66±0.00	93.73±0.00
CEO	72.23	NA	25.95±0.06	70.97±0.00	75.68±0.00

Means and standard deviation. Where rue methanolic extract (RE), metronidazole (MZL), clove essential oil (CEO), not applicable (NA) because 210 nm was specified for RE and 220 nm for CEO.

Degradation of the beads

During the degradation process, there were no significant differences in the weights of the cross-linked microspheres. The microspheres of RE+MZL (11.5 %) degraded at a higher rate than RE (8 %-10 %), similarly CEO+MZL (11.5 %-11.6 %) than CEO (10 %), although the latter had an increase in degradation from day 4 to 6 and that all four treatments had a constant

degradation from day 7 to 14; in acid and basic pH. Moreover, our results had significant differences for treatments ($F=24.53_3$, $p<0.0001$), pH ($F=42.87_1$, $p<0.0001$), and interaction treatment*pH ($F=7.74_3$, $p<0.0005$) and a block as days ($F=14.06_5$, $p<0.0001$), which means that as time goes by, the microsphere matrix degrades over the days, enhanced by the treatments and by the pH (Figure 3). The days were determined for a study realized by Fath-Bayati (2020), where the degradation rate of alginate hydrogel revealed that the loss of gel mass began after three days of test initiation and accelerated between days 7 and 14 (42).

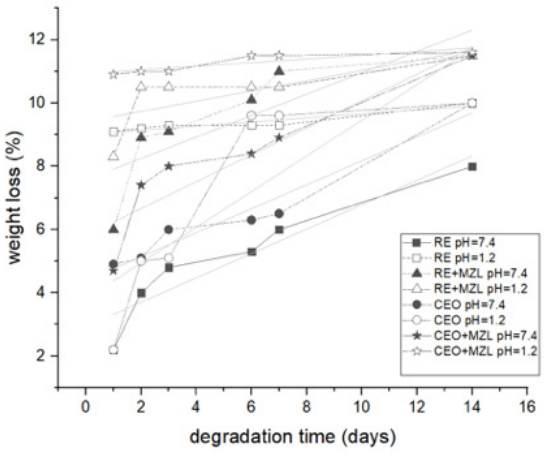

Figure 3. Weight loss average and standard deviation percentage with a linear fit of microspheres of RE, RE+MZL, CEO, and CEO+MZL as a function of degradation time in medium PBS at pH=7.4 and gastric medium (diluted HCl) at pH=1.2. Where n= 3 per treatment.

Release kinetics

Based on the morphological characteristics derived from the images of the microspheres, the encapsulation efficiency and degradation (%), and measurements of the pH of RE and CEO (6 and 5 respectively) were performed. Moreover, the release kinetics of the four treatments were evaluated in PBS at pH=7.4 and with diluted HCl at pH=1.2 at 37 °C from 0 min to 120 min. The cumulative release of RE and RE+MZL at the different wavelengths was 6 %-13 % and 11 %-21 % (Figure 4a), respectively, up to 120 min compared to CEO and CEO+MZL where there were 10 %-61 % and 14 %-68 % (Figure 4c) at acidic pH. In contrast, the cumulative release of RE and RE+MZL at the different wavelengths was 43 %-90 % and 66 %-86 % (Figure 4b), respectively, up to 120 min compared to CEO and CEO+MZL, where there were 45 %-96 % and 60 %-99 % at basic pH (Figure 4d).

The *in vitro* performance of the prepared microspheres showed a sustained release in all four treatments plus CEO. Based on the results, we can conclude that the active substances contained in the CEO and CEO+MZL microspheres were released more than those in RE and RE+MZL. Therefore, the release profile was significantly dependent on the composition of the prepared microspheres. According to our results, a significant factor was the pH of the active ingredients and the microsphere cross-linking and swelling method. The active ingredients can be released within 90-120 min for most chemically and physically cross-linked microspheres.

The profile revealed that the release process was divided into two stages. The first stage was the burst release, which can be attributed to the extract adsorbed on the surface of the microspheres. Furthermore, all four treatments had an initial potential release in the first few minutes. The release remained significantly slower and continuous, and our results were significantly statistically for time ($F=55.637$, $p<0.05$), pH ($F=158.031$, $p<0.05$), wavelength ($F=30.343$, $p<0.05$), and the interaction pH*wavelength ($F=56.593$, $p<0.05$), which means that the release kinetics in each of the treatments is influenced over time by pH and wavelengths as these help us to understand whether some majority secondary metabolites remain present over time or are released.

The release data of the four treatments at both pHs were analyzed with different kinetic models (Table 2). There are two regimes of linear reductions that provide the most suitable models, Korsmeyer-Peppas and Peppas-Sahlin. The kinetic parameters (obtained by equations) gave an n of between 0.10-1.10 (Korsmeyer-Peppas) and an m of 0.13-1.53 (Peppas-Sahlin),

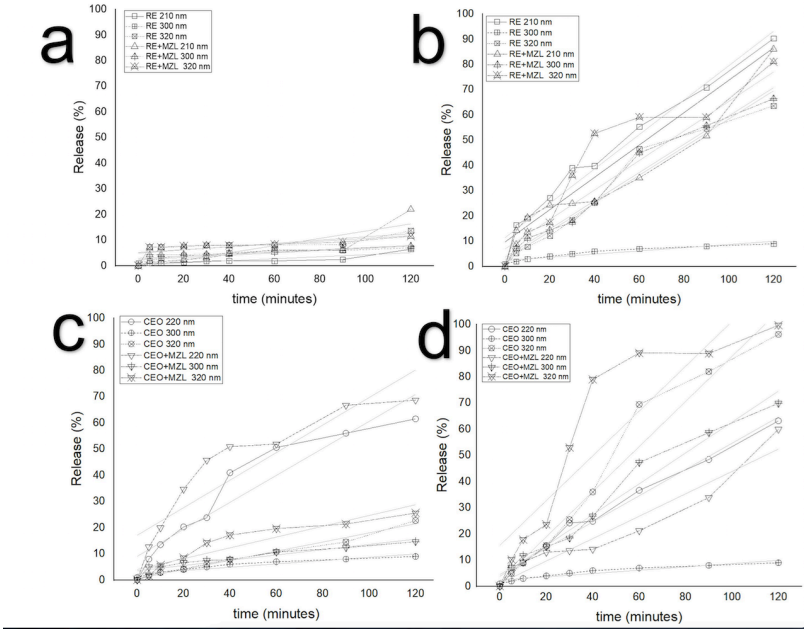

Figure 4. *In vitro* drug release average percentage with standard deviation with a linear fit of microspheres of RE, RE+MZL, CEO, CEO+MZL in PBS medium at pH=7.4 (b, d), and diluted HCl at pH=1.2 (a, b) and 37 ºC. Where n= 3 per treatment.

indicating that the drug transport may be a combination of diffusion-controlled release and swelling and may behave as a Fickian=diffusion type release. In this sense, there was a fractional release due to high swelling. Although exceeding the Korsmeyer-Peppas limit (0.43), the Fickian diffusion of a drug is attributed to the Kd values being much higher than the Kr values, and non-Fickian processes results as Super Case II: n >0.85), for the above mentioned the most appropriate mathematical model for both pHs in all treatments is Korsmeyer-Peppas.

Table 2

Fitting parameters obtained from the mathematical models of Zero order, First order, Korsmeyer-Peppas, Peppas-Sahlin, and Weibull to the experimental data of RE, RE+MZL, CEO, CEO+MZL microspheres drug release

	Zero order				First order				Korsmeyer Peppas				Peppas Sahlin				Weibull			
microspheres	pH 1.2		pH 7.4		pH 1.2		pH 7.4		pH 1.2		pH 7.4		pH 1.2		pH 7.4		pH 1.2		pH 7.4	
	r2	m	r2	m	r2	m	r2	m	r2	K	r2	K	r2	Kd	r2	Kd	r2	m	r2	m
RE 210	0.7914	-0.0392	0.9673	-0.6814	0.7874	-0.0004	0.9401	-0.0171	0.8862	0.0552	0.9956	4.3019	0.8988	0.0839	0.9957	0.0841	0.7183	1.8083	0.8838	0.8518
RE 300	0.6783	-0.0569	0.8560	-0.2836	0.6809	-0.0006	0.8127	-0.0037	0.8218	1.3851	0.9286	0.2213	0.8219	1.3839	0.9268	0.4388	0.7713	1.7274	0.9660	1.1348
RE 320	0.5677	-0.0637	0.9637	-0.5565	0.6828	-0.0004	0.9864	-0.0091	0.9097	4.5836	0.9871	1.3067	0.9110	3.5234	0.9849	2.3484	0.6891	1.3759	0.9822	0.9031
RE+MZL 210	0.7779	-0.1415	0.8854	-0.6408	0.5842	-0.0007	0.8102	-0.0130	0.9520	0.0001	0.9555	1.6389	0.9474	0.0061	0.9552	0.0061	0.8503	1.2141	0.8554	0.9017
RE+MZL 300	0.6699	-0.0419	0.9750	-0.5596	0.7575	-0.0016	0.9813	-0.0088	0.9617	2.4965	0.9907	1.3864	0.7683	0.0061	0.9906	0.0061	0.7846	1.8495	0.9663	0.9237
RE+MZL 320	0.5238	-0.0546	0.9286	-0.5844	0.5422	-0.0006	0.9326	-0.0037	0.9726	5.1469	0.9707	4.1485	0.6484	0.0061	0.9707	0.0061	0.6801	1.3913	0.9390	0.8502
CEO 220	0.7270	-0.6047	0.8560	-0.7166	0.9511	-0.0193	0.6277	-0.0280	0.9510	9.4403	0.9975	3.9114	0.9813	0.0840	0.9975	0.0843	0.8894	0.7331	0.9197	0.7691
CEO 300	0.1834	-0.3239	0.9852	-1.2024	0.3568	-0.0134	0.9413	0.0434	0.8849	2.5313	0.9288	0.5474	0.9914	2.0730	0.9271	0.5342	0.7472	1.0781	0.9230	0.8930
CEO 320	0.2848	-0.4040	0.9355	-1.0256	0.7859	-0.0265	0.8572	-0.0468	0.9994	0.5621	0.9856	3.5641	0.9868	1.6225	0.9854	2.6792	0.9976	0.9871	0.9678	0.6910
CEO+MZL 220	0.8354	-0.5935	0.9648	-2.0668	0.9761	-0.0155	0.8035	-0.0317	0.8793	21.7905	0.9726	0.6327	0.9837	0.0061	0.9720	0.0061	0.8137	0.6809	0.9163	0.8240
CEO+MZL 300	0.2165	-0.3467	0.9751	-1.4142	0.4886	-0.0156	0.8337	-0.0468	0.8672	4.5586	0.9907	3.4856	0.9894	0.0061	0.9906	0.0061	0.8287	1.0453	0.9221	0.7507
CEO+MZL 320	0.3642	-0.4353	0.8109	-2.0519	0.8770	-0.0260	0.5911	-0.0415	0.9385	4.5316	0.9521	17.4673	0.9797	0.0061	0.9521	0.0061	0.9323	0.8419	0.8866	0.6514

Haemocompatibility

The results of the hemolysis assay showed that all tested materials guarantee hemolysis lower than 5 %, except CEO+MZL 5.5 % (Figure 5a). Therefore, according to the ISO standard for medical devices, they can be considered compatible with human red blood

cells; furthermore, RE and RE+MZL could be considered non-hemolytic as their results are less than 2 %, with statistically significant differences between treatments ($F=4709.76_3$, $p<0.0001$). There were no differences in platelet aggregation of the samples compared to the control (saline solution) in the platelet study, with no agglomeration observed. Moreover, rounded morphologies were observed in all micrographs (data not shown). Finally, the leukocyte degranulation test showed a typical cell structure, with no differences in morphology or presence of granules (data not shown).

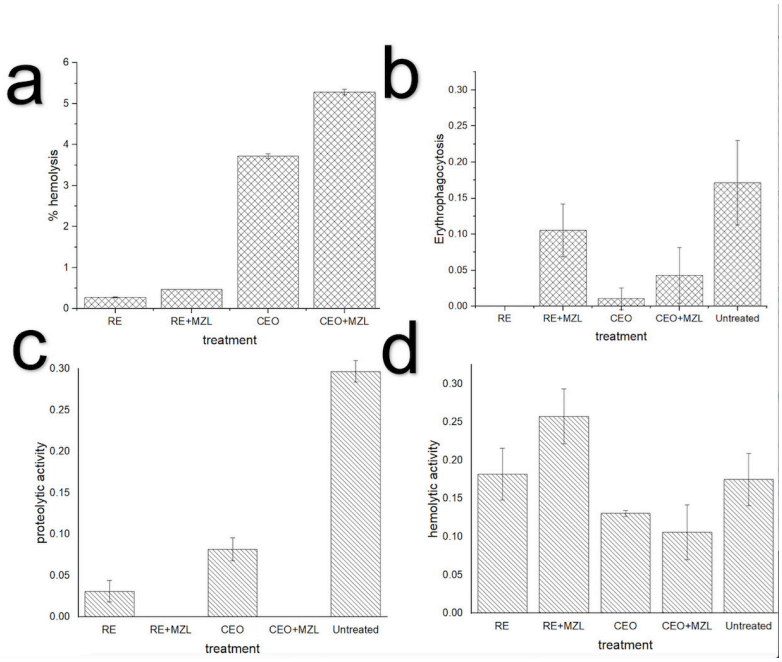

Figure 5. Hemocompatibility (a), parasitic activities; erythrophagocytosis (b), proteolytic activity (c), and hemolytic activity (d).

Erythrophagocytosis, hemolytic activity, and proteolytic activity

Several amoebic functions are necessary for the parasite's virulence, such as proteolytic activity, hemolytic activity, erythrophagocytosis; in this sense, for the four treatments, erythrophagocytosis and proteolytic activity were decreased compared with the untreated group (Figure 5b-5c). There was a significant difference between groups for erythrophagocytosis RE+MZL-CEO ($t=5.27$, $p<0.05$) and RE+MZL-CEO+MZL ($t=10.37$, $p<0.001$), and for proteolytic activity ($t=-7.84$, $p<0.05$) and CEO-CEO+MZL ($t=7.84$, $p<0.05$), and in the case of hemolytic activity, only in the case of RE+MZL was observed an increase for the untreated group (Figure 5d) but without statistical significant differences. In order to corroborate the mechanism is necessary to carried out other studies to elucidate this behavior.

DISCUSSION

In the present work it was found that the RE, RE+MZL, CEO, CEO+MZL microspheres had a sphericity factor equal to one. In addition, our yield % more significant was 70 %, except for CEO (54 %) explained for the concentration of active principle from the formation of alginate-extract/oil emulsion droplet during dripping into the gelling solution (Ca^{+2}). This phenomenon is explained when the droplet requires a minimum mass capable of breaking the surface tension to precipitate its fall (by gravity effect) and release

CO_2 during gelation, which interferes with microsphere dehydration. Similarly, Chan (43) pointed out that the distance between the needle and the surface of the encapsulation medium also plays a role, and the surface of the encapsulation medium and the emulsion loss that occurs during the transfer of the emulsion between the emulsion tube and the syringe. It also depends on the method used to obtain yields equal to or greater than 80 %, such as spray drying or coacervation with solvent evaporation, among others (44-46).

The encapsulation efficiency was read at different wavelengths. The most accurate readings were at 300 and 320 nm due to the secondary metabolites found at these wavelengths. The literature indicated mainly indoles; harmine, harmaline and psoralen, xanthotoxin, bergapten, isopimpinellin in RE and RE+MZL (300 nm), and eugenol in CEO and CEO+MZL (280 nm), as well as at 320 nm with the MZL (47-49). In the case of the CEO and CEO+MZL wavelengths of 220 nm, the proportion of the microsphere formulation can be influenced since increasing the proportion stoichiometrically increases the retention of the active ingredient. Those mentioned above, which in turn affects the EE %, since a high content of essential oil or surface-active ingredient can cause a more significant loss of volatile components due to an unstable formulation as well as affecting their permeability and porosity, creating a low encapsulation efficiency which the pHs of the active ingredients may have influenced creating undesired pregelification (50-53).

In an acidic environment, the carboxylic groups (guluronic acids) of alginate are protonated, which reduces the electrostatic repulsion between the alginate chains and the generation of hydrogen bridges that stabilize the microsphere matrix (54). Moreover, increasing the insolubility and limiting its absorption, in the alkaline medium (intestine), promotes ionic exchange between Ca^{2+} and Na^{+}, resulting in swelling as carboxylic acids ionize and progressive erosion of the microsphere (55). Likewise, for degradation at both pHs, hydrolytic degradation is observed as more time passes with statistical differences between days, pH, and treatments. Furthermore, the weight loss remains constant as shown in a study with Curcuma microspheres were in the time existed degradation (56) with two possible mechanisms such as the incorporation of the aqueous medium into the microsphere and the progressive disintegration by alteration of the calcium alginate matrix.

The release of the microspheres under gastric conditions (pH=1.2) was lower than 22 % for RE and RE+MZL. It is possibly correlated with a low degree of swelling that reduces the porosity and disintegration; or some interaction between the pH of the extract and that of the medium forming some complex causing repulsions of their molecular chains, steric hindrance, or some deprotonation of NH^{+} groups preventing the diffusion of RE and RE+MZL (57,58). On the contrary, for CEO and CEO+MZL, the results indicate stages such as an initial intense release until 60 min, releasing almost half of the compound. After this stage, a slower constant release until reaching the highest release at 120 min in the different wavelengths where the ones with the highest release are those of 220 nm, probably some secondary metabolite is more susceptible to the porosity of the microsphere and is released. In the case of intestinal pH for the four treatments, there was the same phenomenon of the maximum release peak between 60 and 80 min, since, in alkaline media, there is the formation of pores and channels that can facilitate the migration of the active principles (57,58). Similar results to those of this study were found by Dima et al. (59), who determined that the degree of swelling directly affects the release rate of coriander essential oil, limiting its release at the stomach level, and the study of Uyen et al. (56) at the intestinal level.

Additionally, the release of the four treatments showed a good correlation with the Korsmeyer-Peppas and Peppas-Sahlin models. Furthermore, it suggests a relaxation-dissolution mechanism, i.e., diffusion according to Fick's Law and relaxation by swelling of the polymeric structure where those with $r<0.88$ would have a pseudo-fickian behavior associated with the presence of porosity within the polymeric matrix; in addition, having a blast effect in the first minutes due to the diffusion of the active principle on the surface of the matrix (30,60). Similarly, studies of alginate beads with polyelectrolyte layers and magnetic nanocellulose alginate hydrogel beads correlated with the models above (61,62).

In terms of hemocompatibility and biological variables, all treatments had a hemolysis rate of 5 %-10 %, which according to the standards (35), at least with the our results could be a suitable material, as well as not activate the immune system, which could cause thrombi in the case of non-aggregation of platelets and non-disaggregation of leukocytes. However, other activities would have to be evaluated to confirm their safety. In this sense, alginate is considered an anti-thrombogenic material due to its hydrophilicity, which reduces cell adhesion and protein adsorption (63), although it has not been thoroughly studied in controlled *in vitro* studies. Therefore, no immediate concerns were raised regarding the hemocompatibility of alginate or the devices themselves in an *in vitro* setting, and this would require investigations of the immune response with various immune components such as antibodies, other proteins, and immune cells, to monitor adhesion, adsorption, activation, and penetration into the biomaterial (64). In addition, similar studies have shown that the use of alginate as a biomaterial is hemocompatible (64,65).

In regard to biological activities of *E.histolytica*, our objective was that our microspheres would decrease the different activities compared with the untreated group, as these are virulence factors necessary for the survival of the amoeba. The amoeba ingests hemoglobin due to the iron that allows it to lyse erythrocytes and phagocytose them; in addition to its proteolytic activity that allows it to evade the immune system and produce apoptosis in the host cells mediated by cysteine proteases (66). The present results indicate that the treatments decreased erythrophagocytosis and proteolytic activity, in agreement with a study using cysteine proteases, while hemolytic activity was not affected by RE+MZL, similarly to a study of rabeprazole (36). This phenomenon can be explained by an interaction between metronidazole and rue since it was shown that rue and its components protect erythrocytes from oxidative stress and even protect the colon (67).

Thus, the present microspheres could be used as adjuvants in the treatment against *E. histolytica*, in agreement with studies using rue (12,68). Likewise, cloves have antioxidant, anti-inflammatory, and antipyretic properties that do not affect the liver (69-71).

CONCLUSIONS

The microspheres with the four treatments have a yield higher than 50 %, and their encapsulation efficiencies are more preserved in the extract than in the essential oil. Moreover, they have a more constant release rate at pH= 7.4, especially in the extract, the essential oil at both pHs up to 2 h and follow a relaxed-dispersed Korsmeyer-Peppas and Peppas-Sahlin kinetics. Their degradation is constant up to 14 d but faster at acid pH, especially in the essential oil. In addition, there was no platelet activation or degranulation, the % of hemolysis was less than 5 %-10 % being hemocompatible, and their parasitic activity in amoeba virulence factors was diminished when using the treatments in the proteolytic and erythrophagocytic activities. However, the RE+MZL hemolytic activity was not affected.

Therefore, for future work, it is necessary to isolate the majority of products of these plants, reformulate and vary the technique of obtaining the microspheres by adding gum arabic, glycerin, chitosan, and some surfactant, especially in CEO and CEO+MZL so that there is a constant release, as well as to evaluate the swelling kinetics % porosity, prolong the sampling times in the release kinetics and take into account the pHs of the secondary metabolites before pregelification and after. In addition to performing *in vitro* and *in vivo* toxicity tests and complementing with quantifiable tests to evaluate cytokine activation, among others.

Funding/Support: This work was supported by the National Council of Science and Technology National Science scholarship (850039).

Conflicts of interest: The authors report no declarations of interest.

Acknowledgments: We thank Mara Prior-González and the Division of Neurosciences of the Institute of Cell Physiology, UNAM, for donating some reagents for the research.

REFERENCES

1. Parra Huertas RA. Food microencapsulation: A review. RFNAM. 2010;63(2):5669-5684.
2. Shakeel Ahmed, Suvardhan Kanchi GK. Handbook of Biopolymers: Advances and Multifaceted Applications. Pan Stanford Publ. 2018;
3. Pasin BL, González Azón C, Garriga AM. Microencapsulación con alginato en alimentos. Técnicas y aplicaciones Microencapsulation in alginate for food. Technologies and applications. Rev Venez Cienc y Tecnol Aliment. 2012;
4. Avendaño-Romero G, López-Malo A, Paolu E. Propiedades del alginato y aplicaciones en alimentos. TSIA. 2013;7(1):87-96.
5. Pingale PL, Ravindra RP. Comparative study of herbal extract of *Piper Nigrum, Piper Album* and *Piper Longum* on various characteristics of pyrazinamide and ethambutol microspheres. J Drug Deliv Ther. 2019;9(4-A):72-78.
6. Lauro MR, Amato G, Sansone F, Carbone C, Puglisi G. Alginate Carriers for Bioactive Substances: Herbal Natural Compounds and Nucleic Acid Materials. Alginates. 2020;559-604.
7. Mejía-Argueta EL, Santillán-Benítez JG, Flores-Merino MV, Cervantes-Rebolledo C. Herbal extracts and essential oils microencapsulation studies for different applications. J HerbMed Pharmacol. 2021;10(3):289-295.
8. Food and Drug Administration. Use of International Standard ISO 10993-1, "Biological Evaluation of Medical Devices Part 1: Evaluation and Testing within a Risk Management Process". Guidance for Industry and Food and Drug Administration Staff. Food and Drug Administration, Center for Devices and Radiological Health. 2016.
9. Kulkarni GT. Herbal drug delivery systems: An emerging area in herbal drug research. J ChronotherDrug Deliv. 2011;2(3):113-119.
10. Shrivastava S, Gidwani B, Gupta A, Kaur CD. Preparation and characterization of microspheres containing Gallic Acid Adv Pharm J. 2016;1(4):95-100.
11. Niizawa I, Espinaco BY, Zorrilla SE, Sihufe GA. Natural astaxanthin encapsulation: Use of response surface methodology for the design of alginate beads. Int J Biol Macromol. 2019;121:601-608.
12. Bazaldúa-Rodríguez AF, Quintanilla-Licea R, Verde-Star MJ, Hernández-García ME, Vargas-Villarreal J, Garza-González JN. Furanocoumarins from *Ruta chalepensis* with Amebicide Activity. Molecules. 2021;26(12):3684.
13. Anwar A, Ting ELS, Anwar A, Ain N ul, Faizi S, Shah MR. Antiamoebic activity of plant-based natural products and their conjugated silver nanoparticles against *Acanthamoeba castellanii* (ATCC 50492). AMB Express. 2020;10(1).
14. Nezaratizade S, Hashemi N. Ommi D, Orhan IE, Khamesipour F. A systematic review of anti-*Entamoeba histolytica* activity of medicinal plants published in the last 20 years. Parasitology. 2021:1-42.
15. Garcia P, Luna N, Uribarren-Berrueta T. Entamoebosis o Amibiasis o Amebiasis. UNAM. 2016;
16. López Nigro MM, Palermo AM, Mudry MD, Carballo MA. Cytogenetic evaluation of two nitroimidazole derivatives. Toxicol Vitr. 2003;17(1):35-40.
17. Paarakh MP, Jose PA, Setty CM, Christoper GP. Release kinetics–concepts and applications. Int J Pharm ResTechnol. 2018;8(1):12-20.
18. Food and Drug Administration, HHS. International Conference on Harmonisation: Guidance on Q1D Bracketing and Matrixing Designs for Stability Testing of New Drug Substances and Products; Availability. Notice. Federal Register. 2003;68(11):2339-2340.
19. Arianto A, Bangun H, Harahap U, Ilyas S. Effect of alginate chitosan ratio on the swelling, mucoadhesive, and release of ranitidine from spherical matrices of alginate-chitosan. Int J Pharmtech Res. 2015;8(4):653-665.
20. Arianto A, Bangun H, Harahap U, Ilyas S. The comparison of swelling, mucoadhesive, and release of ranitidine from spherical matrices of alginate, chitosan, alginate-chitosan, and calcium alginate-chitosan. Int J Pharmtech Res. 2014;6(7):2054-2063.
21. Wang Y, Guo S, Wang D. Lin Q, Rong L, Zhao J. Resolution enhancement phase-contrast imaging by microsphere digital holography. Opt Commun. 2016;366:81-87.
22. Oliver Urrutia C, Rosales-Ibáñez R, Dominguez García MV, Flores-Estrada J, Flores-Merino M V. Synthesis and assessment of poly(acrylic acid)/ polyvinylpyrrolidone interpenetrating network as a matrix for oral mucosa cells. J Biomater Appl. 2020;34(7):998-1008.
23. Khorshidian N, Mahboubi A, Kalantari N, Hosseini H, Yousefi M, Arab M, et al. Chitosan-coated alginate microcapsules loaded with herbal galactagogue extract: Formulation optimization and characterization. IJPR. 2019;18(3):1180.
24. Zhang X, Dai K, Liu C, Hu H, Luo F, Qi Q, Yang F. Berberine-Coated Biomimetic Composite Microspheres for Simultaneously Hemostatic and Antibacterial Performance. Polymers. 2021;13(3):360.
25. George M, Abraham TE. Polyionic hydrocolloids for the intestinal delivery of protein drugs: Alginate and

chitosan—a review. J Control Release. 2006;114(1):1-14.

26. Silva CM, Ribeiro AJ, Figueiredo IV, Gonçalves AR, Veiga F. Alginate microspheres prepared by internal gelation: Development and effect on insulin stability. Int J Pharm. 2006;311(1-2):1-10.
27. Cordoba Villalobos JA, Arriola Peñalosa MA. Farmacopea de los Estados Unidos Mexicanos. 2011.
28. Singhvi G, Singh M. *In-vitro* drug release characterization models. Int J Pharm Stud Res. 2011;2(1):77-84.
29. Shah JC, Deshpande A. Kinetic modeling and comparison of *in vitro* dissolution profiles. WJPS. 2014:302-309.
30. Baggi RB, Kilaru NB. Calculation of predominant drug release mechanism using Peppas-Sahlin model, Part-I (substitution method): A linear regression approach. AJPTech. 2016;6(4):223-230.
31. Lee JS, Choi , Han J. Mathematical modeling of cinnamon (*Cinnamomum verum*) bark oil release from agar/PVA biocomposite film for antimicrobial food packaging: The effects of temperature and relative humidity. Food Chem. 2021;130306.
32. Corsaro C, Neri G, Mezzasalma AM, Fazio E. Weibull Modeling of Controlled Drug Release from Ag-PMA Nanosystems. Polymers. 2021;13(17):2897.
33. Kobryń J, Sowa S, Gasztych M, Dryś A, Musiał W. Influence of hydrophilic polymers on the β factor in weibull equation applied to the release kinetics of a biologically active complex of aesculus hippocastanum. Int J Polym Sci. 2017;2017.
34. Comisión Permanente de la Farmacopea de los Estados Unidos Mexicanos. Farmacopea Herbolaria de los Estados Unidos Mexicanos. 2013.
35. Seyfert UT, Biehl V, Schenk J. *In vitro* hemocompatibility testing of biomaterials according to the ISO 10993-4. Biomol Eng. 2002;19(2–6):91–6.
36. Martínez-Pérez Y, Nequiz-Avendaño M, García-Torres I, Gudiño-Zayas ME, López-Velázquez G, Enríquez-Flores S, et al. Rabeprazole inhibits several functions of *Entamoeba histolytica* related with its virulence. Parasitol Res. 2020;119(10):3491-502.
37. Ramos E, Olivos-García A, Nequiz M, Saavedra E, Tello E, Saralegui A, et al. *Entamoeba histolytica*: apoptosis induced *in vitro* by nitric oxide species. Exp. Parasitol. 2007;116(3):257-265.
38. da Silva Campelo M, Melo EO, Arrais SP, do Nascimento FBSA, Gramosa NV, de Aguiar Soares S, et al. Clove essential oil encapsulated on nanocarrier based on polysaccharide: A strategy for the treatment of vaginal candidiasis. Colloids Surf, A Physicochem Eng Asp. 2021;610:125732.
39. Piletti R, Bugiereck AM, Pereira AT, Gussati E, Dal Magro J, Mello JMM, et al. Microencapsulation of eugenol molecules by β-cyclodextrin as a thermal protection method of antibacterial action. Mater Sci Eng C. 2017;75:259-271.
40. Radomski FAD, de Araujo Duarte C, Ribeiro E, de Sá EL. Optical Investigation of Essential Oils Using Absorbance and Photoluminescence. Appl Spectrosc. 2021;75(9):1136-1145.
41. Van Hung T, Alkhamis HH, Alrefaei AF, Sohret Y, Brindhadevi K. Prediction of emission characteristics of a diesel engine using experimental and artificial neural networks. Appl Nanosci. 2021:1-10.
42. Fath-Bayati, L, Ai J. Assessment of mesenchymal stem cell effect on foreign body response induced by intraperitoneally implanted alginate spheres. J Biomed Mater Res A. 2020;108(1):94-102.
43. Chan ES. Preparation of Ca-alginate beads containing high oil content: Influence of process variables on encapsulation efficiency and bead properties. Carbohydr Polym. 2011;84(4):1267-1275.
44. Banerjee S, Chattopadhyay P, Ghosh A, Goyary D, Karmakar S, Veer V. Influence of process variables on essential oil microcapsule properties by carbohydrate polymer–protein blends. Carbohydr Polym. 2013;93(2):691-697.
45. Kopp VV, Agustini CB, dos Santos JHZ, Gutterres M. Microencapsulation of clove essential oil with gelatin and alginate. XXXV Congress of IULT CS, Dresden. 2019;164:1-9.
46. Kumar R, Kumar Shrivastava S. Formulation, Development and Characterization of Floating Microspheres of Selected Calcium Channel Blocker.
47. Milesi S, Massot B, Gontier E, Bourgaud F, Guckert A. *Ruta graveolens* L. a promising species for the production of furanocoumarins. Plant Sci. 2001;161(1):189-199.
48. Trivedi MK, Patil S, Shettigar H, Bairwa K, Jana S. Spectroscopic characterization of biofield treated metronidazole and tinidazole. Med Chem. 2015;5(7):340-344.
49. Das A, Harshadha K, Dhinesh Kannan SK, Hari Raj K, Jayaprakash B. Evaluation of therapeutic potential of eugenol-a natural derivative of Syzygium aromaticum on cervical cancer. APJCP. 2018;19(7):1977.
50. Planas M, Fernández-Reiriz MJ, Ferreiro MJ, Labarta U. Effect of selected variables on the preparation of gelatin-acacia microcapsules for aquaculture. Aquac Eng. 1990;9(5):329-341.
51. Pedroza-IslasR, Vernon-Carter EJ, Durán-Domınguez C, Trejo-Martınez S. Using biopolymer blends for shrimp feedstuff microencapsulation—I. Microcapsule particle size, morphology and microstructure. Food Res Int. 1999;32(5):367-374.
52. Bringas-Lantigua M, Valdés D, Pino JA. Influence of spray-dryer air temperatures on encapsulated lime

essential oil. Int J Food Sci Technol. 2012;47(7):1511-1517.

53. Rodea-González DA, Cruz-Olivares J, Román-Guerrero A, Rodríguez-Huezo ME, Vernon-Carter EJ, Pérez-Alonso C. Spray-dried encapsulation of chia essential oil (*Salvia hispanica* L.) in whey protein concentrate-polysaccharide matrices. J Food Eng. 2012;111(1):102-109.
54. Dima C, Cotârlet M, Alexe P, Dima S. Microencapsulation of essential oil of pimento [*Pimenta dioica* (L) Merr.] by chitosan/k-carrageenan complex coacervation method. IFSET. 2014;22:203-211.
55. dos Santos Silva M, Cocenza DS, Grillo R, de Melo NFS, Tonello PS, de Oliveira LC, et al. Paraquat-loaded alginate/chitosan nanoparticles: preparation, characterization and soil sorption studies. J Hazard Mater. 2011;190(1-3):366-374.
56. Uyen NTT, Hamid ZAA, Ahmad NB. Synthesis and characterization of curcumin-loaded alginate microspheres for drug delivery. J Drug Deliv Sci Technol. 2020;58:101796.
57. Amadi CN, Mgbahurike AA. Selected Food/Herb-Drug Interactions: Mechanisms and Clinical Relevance. Am J Ther. 2018;25(4):e423-e433.
58. Sun X. Liu C, Omer AM, Yang LY, Ouyang XK. Dual-layered pH-sensitive alginate/chitosan/kappa-carrageenan microbeads for colon-targeted release of 5-fluorouracil. Int J Biol Macromol. 2019;132:487-494.
59. Dima C, Pătraşcu L, Cantaragiu A, Alexe P, Dima Ş. The kinetics of the swelling process and the release mechanisms of *Coriandrum sativum* L. essential oil from chitosan/alginate/inulin microcapsules. Food Chem. 2016;195:39-48.
60. Rezaei A, Nasirpour A, Tavanai H, Fathi M. A study on the release kinetics and mechanisms of vanillin incorporated in almond gum/polyvinyl alcohol composite nanofibers in different aqueous food simulants and simulated saliva. Flavour Fragr J. 2016;31(6):442-447.
61. Supramaniam J, Adnan R, Kaus NHM, Bushra R. Magnetic nanocellulose alginate hydrogel beads as potential drug delivery system. Int J Biol Macromol. 2018;118:640-648.
62. Witzler M, Vermeeren S, Kolevatov RO, Haddad R, Gericke M, Heinze T. Evaluating Release Kinetics from Alginate Beads Coated with Polyelectrolyte Layers for Sustained Drug Delivery. ACS Appl Bio Mater. 2021;4(9):6719-6731.
63. de Vos P, Faas MM, Strand B, Calafiore R. Alginate-based microcapsules for immunoisolation of pancreatic islets. Biomaterials. 2006;27(32):5603-5617.
64. Fernandez SA, Danielczak L, Gauvin-Rossignol G, Hasilo C, Bégin-Drolet A, Ruel J, Hoesli CA. An *in vitro* perfused macroencapsulation device to study hemocompatibility and survival of islet-like cell clusters. Front Bioeng Biotechnol. 2021;9.
65. Mohammadpour M, Samadian H, Moradi N, Izadi Z, Eftekhari M, Hamidi M, Elboutachfaiti R. Fabrication and Characterization of Nanocomposite Hydrogel Based on Alginate/Nano-Hydroxyapatite Loaded with Linum usitatissimum Extract as a Bone Tissue Engineering Scaffold Mar Drugs. 2022;20(1):20.
66. Navarrete-Mena A, Pacheco-Yépez J, Hernández-Ramírez VI, Escalona-Montaño AR, Gómez-Sandoval JN, Néquiz-Avendaño M, et al. Protein Phosphatase PP2C Identification in *Entamoeba spp*. BioMed Res Internat. 2021.
67. Licata A, Licata E, Vanella A, Malaguarnera M. Oxidative profile in patients with colon cancer: effects of *Ruta chalepensis* L. Eur Rev Med Pharmacol Sci. 2011;15:181-191.
68. Nahar L, Al-Majmaie S, Al-Groshi A, Rasul A, Sarker SD. Chalepin and chalepensin: Occurrence, biosynthesis and therapeutic potential. Molecules. 2021;26(6):1609.
69. Uchôa Lopes CM, Saturnino de Oliveira JR, Holanda VN, Rodrigues AYF, Martins da Fonseca CS, Galvão Rodrigues FF, et al. Analysis and Hemolytic, Antipyretic and Antidiarrheal Potential of *Syzygium aromaticum* (Clove) Essential Oil. Separations. 2020;7(2):35.
70. Das M, Roy S, Guha C, Saha AK, Singh M. *In vitro* evaluation of antioxidant and antibacterial properties of supercritical CO_2 extracted essential oil from clove bud (*Syzygium aromaticum*). J Plant Biochem Biotechnol. 2020:1-5.
71. Kasyap K, Yesudanam S, Prasanth ML, Prasanth CS. An *in-vitro* anti-inflammatory activity of hydroalcoholic extracts and essential oil of Syzygium aromaticum. Int J Med Pharm Case Reports. 2021:33-39.